Performance of the K^+ ion diode in the 2 MV injector for heavy ion fusion

F. M. Bieniosek,[a] E. Henestroza, and J. W. Kwan
Lawrence Berkeley National Laboratory, Berkeley, California 94720

(Presented on 6 September 2001)

Heavy ion beam inertial fusion driver concepts depend on the availability and performance of high-brightness high-current ion sources. Surface ionization sources have relatively low current density but high brightness because of the low temperature of the emitted ions. We have measured the beam profiles at the exit of the injector diode, and compared the measured profiles with EGUN and WARP-3D predictions. Spherical aberrations are significant in this large aspect ratio diode. We discuss the measured and calculated beam size and beam profiles, the effect of aberrations, quality of vacuum, and secondary electron distributions on the beam profile. © *2002 American Institute of Physics.* [DOI: 10.1063/1.1428417]

I. INTRODUCTION

A typical heavy ion fusion driver concept has about 100 parallel beam channels with each channel transporting a beam of line charge density 0.25 μC/m. An ESQ injector,[1] representing a single driver beam, has been in operation at Lawrence Berkeley National Laboratory. Initially the injector produced a beam with adequate current and emittance, but with a hollow intensity profile at the end of the ESQ section. Recent work on the injector has centered on studying the behavior of the beam in the source and diode regions, and preparing the injector for the High Current Experiment (HCX).[2]

Careful attention to beam parameters in the diode is essential to understanding downstream beam behavior. Specific issues include a comparison between measured and predicted beam current, beam size, beam profiles, and uniformity of emission.

II. EQUIPMENT AND DIAGNOSTICS

Figure 1 shows a cross-sectional view of the injector. The injector is contained inside a pressure vessel that houses the Marx generator, the high voltage dome containing the ion source and electronics, and the ESQ transport and accelerating section. Only the diode section was energized in the measurements discussed here. The injector diode is typically operated as a triode, in which the extracting electrode acts as a switch. To achieve a fast rise time, beam extraction is performed during the Marx generator flattop by pulsing the source voltage positive with respect to the dome and extraction electrode. The beam pulse has recently been lengthened from 2.0 to 4.5 μs.

The source is a 10-cm-diam spherically curved, hot porous-tungsten contact ionizer source at a temperature of about 1100 °C. Maximum beam current density is space-charge limited to approximately 10 mA/cm^2. Two types of ion sources were used in this investigation: a K^+ aluminosilicate source, and a K^+ contact ionizer source.[3] The aluminosilicate source was prepared by melting a thin layer of aluminosilicate material $K_2O{\bullet}Al_2O_3{\bullet}4SiO_2$, which is a synthetic analog of the zeolite spodumene, to form a smooth coating on the porous tungsten substrate of the source. The contact ionizer source was prepared by applying a solution of K_2CO_3 on the bare porous tungsten substrate. Baking at a temperature in excess of 500 °C dissociates the carbonate, and releases CO and CO_2. The potassium atoms are avail-

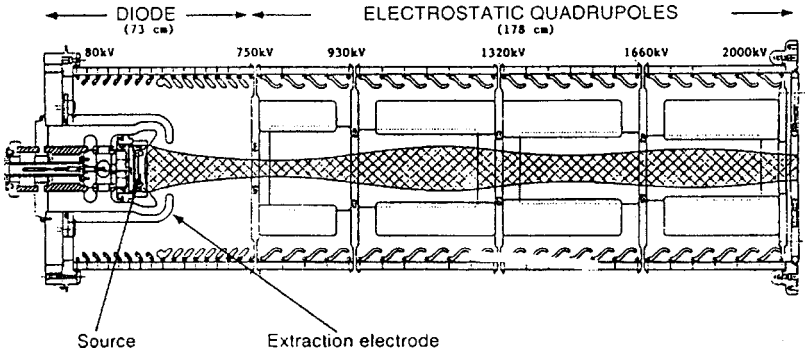

FIG. 1. Cross-sectional view of the injector.

[a]Electronic mail: fmbieniosek@lbl.gov

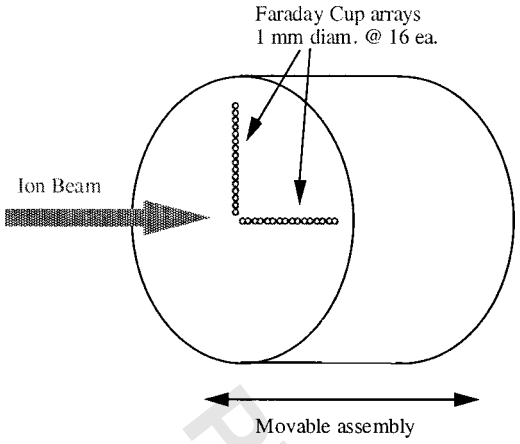

FIG. 2. Schematic diagram of the 32-channel Faraday cup array.

able for emission as ions, and the remaining oxygen atoms can affect the work function of the source surface. A long-term solution based on this approach is to provide a continuous feed of potassium ions.

The beam properties were found to be sensitive to vacuum conditions. In particular, measurements made under poor vacuum conditions tended to show spurious results, such as a large central spike in the beam profiles. Poor vacuum can affect beam conditions by creation of secondary electron distributions in the beam, and by charge-exchange of beam ions. As a result, the operating pressure near the source was reduced, by improved vacuum technique and replacement of a graphite Pierce electrode with a water-cooled copper electrode, from the mid 10^{-5} Torr range to the mid 10^{-7} Torr range.

The injector diode is instrumented with a large Faraday cup for beam current measurements, kapton films for beam image patterns, and a multiple Faraday cup array (FCA). The FCA consists of an array of small Faraday cups arranged in two orthogonal rows mounted in a single movable assembly. The collectors are staggered in radius with a center-to-center separation of 3.8 mm. The assembly can be rotated and translated along the beam axis inside the ESQ column. Figure 2 shows the configuration of the collectors. It was found necessary for proper operation of the FCA to take precautions to prevent infiltration into the beam of secondary electrons created at the end plate of the diagnostic array.

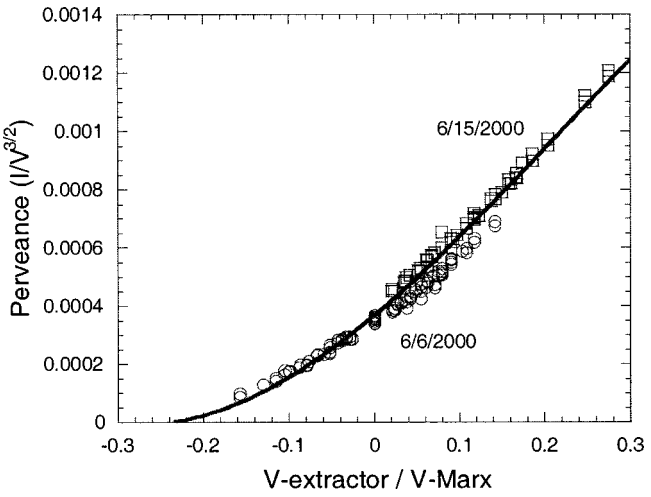

FIG. 3. Comparison between measured and predicted (EGUN) beam current in the diode for the 10-cm-diam aluminosilicate source. Dates of measurements are indicated.

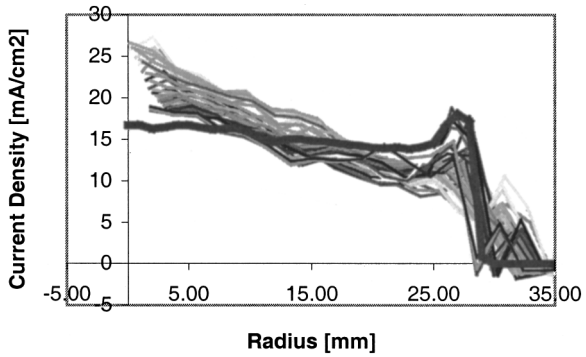

FIG. 4. Measured beam profiles for an 80 kV equivalent (extractor) beam at an axial distance of 2.54 cm, and EGUN predicted profile (thick black curve).

III. BEAM MEASUREMENTS

Measurements of the beam perveance ($I/V^{3/2}$) made with a large Faraday cup at the end of the diode are shown in Fig. 3. These are measurements of the beam current as the accelerating voltage [V-Marx] and the extraction voltage [V-extractor] were varied over as wide a range as possible. The actual measured beam currents in this study were in a very wide range, from 27 to 764 mA, as accelerating voltages ranged from 240 to 706 kV. They show good agreement with the EGUN simulation, as shown. The agreement provides clear evidence that the diode was operating at the space-charge limit over a wide operating range.

A series of two-dimensional scans of the beam profile at the exit of the diode were made. Beam current density measurements were taken at 36 angular positions and 16 radial positions to create the map. All 36 radial profiles for a scan under typical operating condition are shown in Fig. 4. The general features of the beam profiles are correctly modeled (including the beam size and the presence of a raised rim,

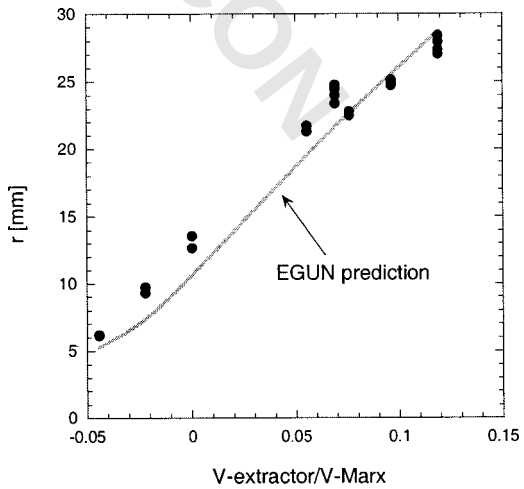

FIG. 5. RMS beam sizes $2\langle x^2\rangle^{1/2}$ and $2\langle y^2\rangle^{1/2}$ for measured beam profiles, compared to EGUN predictions.

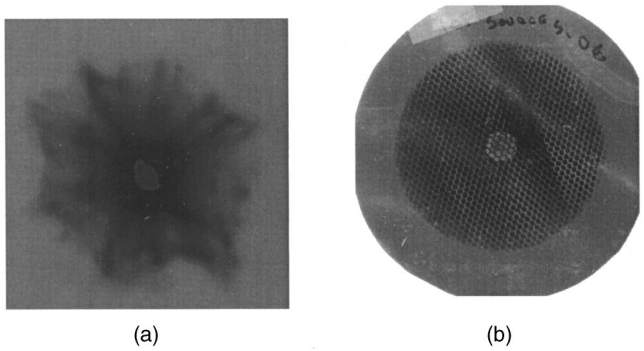

FIG. 6. Kapton images of beam. Each image represents exposure to about 200 beam pulses. (a) Kapton film unshielded, (b) film installed at the collector of the large Faraday cup, behind an electron trap and a honeycomb screen. The nearly vertical streaks are due to imperfections in the honeycomb material.

which is produced in the EGUN simulation by aberrations at the interface between the outer edge of the source and the Pierce electrode). However some details of the profiles, in particular the slope of the distribution, are not accurately reproduced. Note that there is some angular variation in beam profiles, as shown in Fig. 4. In addition, even when the total beam current remained constant, there were some variations from scan to scan, which could be instrumental effects, a manifestation of changes in vacuum properties at the diode, or thermal drift of mechanical components of the diode.

A summary of RMS beam sizes is shown in Fig. 5, and compared with EGUN prediction of RMS beam size at the same axial location. The measured and calculated beam sizes follow the same trend. The residual disagreements may be related to disagreement in the current density profile, or other effects, as noted previously.

Finally, to indicate the sensitivity of the high-space-potential ($\sim$5 kV) heavy ion beam to the presence of secondary electrons, which may be introduced by perturbing diagnostics or by poor vacuum, two images of the beam on kapton film are shown in Fig. 6. On the left-hand side is the image for a bare kapton film, and on the right-hand side is the image for a kapton film behind an electron trap and a honeycomb grid. The dramatic loss of symmetry in the beam profile on the left-hand side is attributed to the effect of secondary electrons on the internal potential distribution of the beam when the kapton is not properly shielded to prevent the release of secondary electrons into the beam.

IV. DISCUSSION

Because of the relatively low current density of these solid-state sources, beam brightness is strongly dependent on emittance growth driven by aberrations in the diode and ESQ regions. Measurements show normalized emittance growth from that only due to the temperature of the source, to emittance measured at the end of the ESQ, of a factor of 4 or greater.[4] Emittance growth is due to several factors. It occurs in the diode, from aberration-driven nonuniformity in the beam profile, especially the high-density rim at the edge of the beam. It also occurs in the ESQ section, predominantly due to the energy effect and image charges on the ESQ electrodes. Further emittance growth can occur due to the nonlinear electrostatic field energy of the nonuniform beam density distribution. WARP-3D simulations indicate that the ESQ dominates emittance growth. The ESQ has been redesigned to reduce emittance growth by reducing radial excursions of the beam. Unfortunately it was not possible to separate the relative contributions of the diode and ESQ to emittance growth in the experiment because of the lack of emittance measurements at the end of the diode. In the future, a pepper-pot diagnostic will be installed to measure beam divergence and emittance growth in the diode.

ACKNOWLEDGMENT

This work was supported by DOE, Office of Fusion Science, under DOE Contract No. DE-AC03-76F00098.

[1] S. S. Yu *et al.*, Fusion Eng. Des. **32-33**, 309 (1996).
[2] S. Lund *et al.*, Proceedings of the 2001 Particle Accelerator Conference, Paper No. RPAH037.
[3] J. W. Kwan, Nucl. Instrum. Methods Phys. Res. A **415**, 268 (1998).
[4] F. M. Bieniosek *et al.*, Proceedings of the 2001 Particle Accelerator Conference, Paper No. WPAH011.